Impact of rice *GENERAL REGULATORY FACTOR14h* (*GF14h*) on low-temperature seed germination and its application to breeding

Yusaku Sugimura[1], Kaori Oikawa[1], Yu Sugihara[2,¤a], Hiroe Utsushi[1], Eiko Kanzaki[1], Kazue Ito[1], Yumiko Ogasawara[1], Tomoaki Fujioka[3], Hiroki Takagi[1,¤b], Motoki Shimizu[1], Hiroyuki Shimono[4,5], Ryohei Terauchi[1,2], Akira Abe[1]

[1] Iwate Biotechnology Research Center, Kitakami, Iwate, Japan

[2] Crop Evolution Laboratory, Kyoto University, Muko, Kyoto, Japan

[3] Iwate Agricultural Research Center, Kitakami, Iwate, Japan

[4] Faculty of Agriculture, Iwate University, Morioka, Iwate, Japan

[5] Agri-Innovation Center, Iwate University, Morioka, Iwate, Japan

[¤a] Current address: The Sainsbury Laboratory, University of East Anglia, Norwich, United Kingdom

[¤b] Current address: Faculty of Bioresources and Environmental Science, Ishikawa Prefectural University, 1-308, Suematsu, Nonoichi, Ishikawa, 921-8836, Japan

* Corresponding author

E-mail: a-abe@ibrc.or.jp (AA)

ORCIDs

Yusaku Sugimura, 0000-0001-7271-7703

Yu Sugihara, 0000-0001-6042-1091

Hiroki Takagi, 0000-0002-8576-9892

Motoki Shimizu, 0000-0002-5622-5554

Hiroyuki Shimono, 0000-0002-7328-0483

Ryohei Terauchi, 0000-0002-0095-4651

Akira Abe, 0000-0002-0344-2643

Abstract

Direct seeding is employed to circumvent the labor-intensive process of rice (*Oryza sativa*) transplantation, but this approach requires varieties with vigorous low-temperature germination (LTG) when sown in cold climates. To investigate the genetic basis of LTG, we identified the quantitative trait locus (QTL) *qLTG11* from rice variety Arroz da Terra, which shows rapid seed germination at lower temperatures, using QTL-seq. We delineated the candidate region to a 52-kb interval containing *GENERAL REGULATORY FACTOR14h* (*GF14h*) gene, which is expressed during seed germination. The Arroz da Terra *GF14h* allele encodes functional GF14h, whereas Japanese rice variety Hitomebore harbors a 4-bp deletion in the coding region. Knocking out functional *GF14h* in a near-isogenic line (NIL) carrying the Arroz da Terra allele decreased LTG, whereas overexpressing functional *GF14h* in Hitomebore increased LTG, indicating that *GF14h* is the causal gene behind *qLTG11*. Analysis of numerous Japanese rice accessions revealed that the functional *GF14h* allele was lost from popular varieties during modern breeding. We generated a NIL in the Hitomebore background carrying a 172-kb genomic fragment from Arroz da Terra including *GF14h*. The NIL showed superior LTG compared

to Hitomebore, with otherwise comparable agronomic traits. The functional *GF14h* allele from Arroz da Terra represents a valuable resource for direct seeding in cold regions.

Author Summary

Rice serves as a fundamental crop sustaining over half of the global population. With the rapid growth of the world's population, it will become increasingly important to improve rice productivity. On the other hand, the aging of rice farmers in Japan has resulted in a constant labor shortage. To address this, direct seeding, in which seeds are sown directly in rice fields without going through the most labor-intensive part of the rice cultivation process, i.e., seedling production and transplanting, has been recommended. However, prevalent elite rice varieties are known to be unsuitable for direct seeding due to their poor seed germination ability under low-temperature conditions. In this study, we show for the first time that *GF14h* gene from the Portuguese variety Arroz da Terra improves seed germination at low temperatures (LTG). In addition, a novel cross-bred line was generated by introducing the *GF14h*-containing genomic segment from Arroz da Terra into Hitomebore, a widely cultivated variety in northern Japan. This line is expected to be used as a pre-breeding material to enhance LTG. This study will provide a genetic basis for LTG and contribute to basic and applied research progress.

Introduction

Low-temperature seed germination (LTG) is a pivotal agronomic trait in rice (*Oryza sativa*). As rice originated from tropical and subtropical regions, it is highly susceptible to low-temperature conditions compared to other cereal crops such as wheat (*Triticum*

aestivum) and barley (*Hordeum vulgare*) [1]. Nevertheless, rice is produced in temperate and high-altitude regions, where it frequently experiences temperatures below 20°C. In Japan, rice is abundantly cultivated in relatively cold areas such as Tohoku and Hokkaido. In recent years, there has been an increasing demand to shift from conventional transplantation-based rice cultivation to direct seeding to reduce labor and costs. However, direct seeding raises the risk of exposure to low temperatures during seed germination [2]. Therefore, to expand the use of direct seeding, it is crucial to breed rice cultivars with enhanced LTG.

LTG is a quantitative trait regulated by complex molecular mechanisms. Linkage mapping and genome-wide association studies (GWAS) have identified over 30 LTG-related quantitative trait loci (QTLs) or genomic regions associated with this trait, located on all 12 rice chromosomes [3-20]. However, only a few genes involved in LTG have been described, such as *qLTG3-1* [3] and *STRESS-ASSOCIATED PROTEIN16* (*OsSAP16*) [15]. The *qLTG3-1* gene, encoding a protein of unknown function, has a substantial influence on LTG [3]. During seed germination, *qLTG3-1* expression is strongly induced in embryos, which leads to the loosening of the tissues covering the embryo by promoting vacuolation [3]. *OsSAP16* encodes a stress-associated protein with two AN1-C2H2 zinc finger domains [15]. OsSAP16 presumably acts as a regulator of LTG.

14-3-3 proteins are regulatory proteins that are widely conserved in eukaryotes. These proteins bind to phosphorylated serine and tyrosine residues in their target proteins that participate in signal transduction and the regulation of gene expression [21, 22], thus altering their enzymatic activity, subcellular localization, stability, or protein–protein interactions [23-25]. The rice genome encodes eight 14-3-3 proteins, named GF14a–h for

95 GENERAL REGULATORY FACTOR14 [26]. *GF14h* is involved in rice seed
96 germination under optimal temperature conditions [27, 28]. In addition, GF14h
97 contributes to phytohormone signaling, including abscisic acid and gibberellin signaling
98 [27, 28]. However, it remains unclear whether *GF14h* promotes seed germination under
99 low-temperature conditions [28].

100 QTL pyramiding has been proposed as a breeding concept [29] for bringing
101 together several QTLs (or genes) related to agronomically important traits in the genetic
102 background of locally adapted elite cultivars. In practice, it is essential to generate pre-
103 breeding materials for QTL pyramiding, i.e., near-isogenic lines (NILs) that harbor one
104 or a few genomic segments introgressed from the donor parent into the genome of the
105 recipient parent through a combination of continuous backcrossing and selfing via
106 marker-assisted selection [30]. In this study, we determined that *GF14h* is responsible for
107 an LTG-related QTL in Portuguese rice variety Arroz da Terra. We generated a NIL in the
108 background of rice cultivar Hitomebore, which is adapted for growth in northern Japan,
109 by replacing its *GF14h* genomic fragment with that from Arroz da Terra and tested its
110 LTG performance.

111

112

113 # Results

114 ## Evaluation of QTLs associated with low-temperature germination using
115 ## the Portuguese rice variety Arroz da Terra

116 We investigated seed germination characteristics of a Portuguese rice variety Arroz da
117 Terra and a Japanese varieties Iwatekko and Hitomebore. Under low-temperature

conditions (15ºC), Arroz da Terra exhibited significantly higher germination rates compared to Iwatekko and Hitomebore during days 7−15, particularly showing a 30−40% increase in germination rate 10−11 days after imbibition (Fig 1A and 1B). Similarly, at normal temperature conditions (25ºC), Arroz da Terra showed superior germination rates 2−4 days after imbibition, especially with a 30% difference observed 3 days after imbibition (Fig 1A and 1C). These findings indicate that Arroz da Terra exhibits more vigorous germination under normal and low-temperature conditions than the Japanese cultivars Iwatekko and Hitomebore. To identify the genes responsible for this difference, we searched for QTLs involved in the high LTG of Arroz da Terra. We previously generated a set of 200 RILs at the F_7 generation derived from a cross between Arroz da Terra and Iwatekko (S1 Fig) [31]. We phenotyped all RILs for LTG at 13ºC and selected the 20 RILs with the highest LTG and the 20 RILs with the lowest LTG. We assembled two pools of seedlings with low or high LTG and extracted their genomic DNA for whole-genome sequencing on the Illumina platform (S1 Fig) [31]. We mapped the resulting sequencing reads to the Nipponbare rice reference genome (IRGSP-1.0) and performed QTL-seq analysis using our new high-performance pipeline [32]. Based on the ΔSNP index, we identified three QTLs related to LTG on chromosome 3 (*qLTG3-1* and *qLTG3-2*) and chromosome 11 (*qLTG11*) (Fig 1D), which is consistent with the results of a previous study [31].

The *qLTG3-1* region contained the gene Os03g0103300, which was reported to be involved in LTG in a study using rice cultivar Italica Livorno, which has high LTG, and Hayamasari, which has low LTG [3]. An examination of its coding sequences in Arroz da Terra, as well as Iwatekko and Hitomebore, revealed that they were identical to those

found in Italica Livorno and Hayamasari, respectively (S2 Fig). While Italica Livorno harbored a functional haplotype for this gene, Hayamasari carried a loss-of-function haplotype due to a 71-bp deletion (S2 Fig) [3]. Therefore, we propose that the causal gene for the QTL *LTG3-1* is Os03g0103300.

To evaluate the contribution of the two other QTLs to LTG, we generated NILs harboring a segment from the Arroz da Terra genome for each QTL (approximately 5 Mb) in the Hitomebore background (Fig 1E; S3A and S4A Figs). We detected no clear effect of *qLTG3-2* on LTG, as *qLTG3-2*-NIL and Hitomebore showed similar seed germination rates at 15ºC (S4B Fig). By contrast, *qLTG11*-NIL showed a significantly higher rate of germination than Hitomebore 7−12 days after imbibition at 15ºC, particularly after 8 and 9 days, showing a difference of more than 40% (Fig 1E and 1F), indicating that *qLTG11* enhances LTG. *qLTG11*-NIL seeds also germinated more rapidly than Hitomebore seeds under normal conditions (25ºC), although with a smaller difference between the two genotypes than at low temperature (S5 Fig). We therefore focused our analysis on *qLTG11*.

Identification of *GF14h* as the candidate gene for *qLTG11*

To delineate the *qLTG11* region, we carried out map-based cloning using a segregating population derived from a cross between BC_2F_3 line *qLTG11*-NIL and Japanese elite cultivar Hitomebore (S3A Fig). For mapping, we conducted germination tests at 15°C. We narrowed down the genomic region containing the QTL to a 52-kb segment (from 23.512 bp to 23.564 Mb) on chromosome 11 based on the Nipponbare reference genome (IRGSP-1.0) (Fig 2A). This interval contains two annotated genes based on the Nipponbare genome sequence (Fig 2B). We compared the genomic sequence of Hitomebore and Arroz da Terra across the candidate region using *de novo* genome

165 assembly obtained from Nanopore long reads. The cultivars Hitomebore and Nipponbare
166 had an identical genomic sequence over the entire candidate region (S6A Fig). By contrast,
167 the genome sequence from Arroz da Terra was substantially different from that of
168 Nipponbare, with the equivalent candidate region spanning approximately 94 kb (Fig 2B
169 and S6B Fig).

170 As the causal gene behind the variation in LTG is likely expressed in seeds, we
171 performed transcriptome deep sequencing (RNA-seq) during seed germination in
172 Hitomebore and *qLTG11*-NIL (S1 Table). Within the candidate region, the gene
173 Os11g0609600, corresponding to the *14-3-3* gene *GF14h*, was expressed in both
174 Hitomebore and *qLTG11*-NIL, whereas Os11g0609500 (*Jacalin-like lectin domain*
175 *containing protein*) was not expressed in seeds (S7 Fig), thus suggesting that *GF14h* is a
176 strong candidate gene for LTG. The *GF14h* gene structure and haplotypes in Arroz da
177 Terra and Hitomebore are shown in Fig 2C. We detected a 4-bp deletion in the *GF14h*
178 coding region in Hitomebore, causing a frameshift mutation predicted to introduce a
179 premature stop codon (Fig 2C and S8 Fig). These results suggest that Hitomebore carries
180 a loss-of-function allele of *GF14h*. To assess the role of *GF14h* in LTG, we examined the
181 expression pattern of the putative functional *GF14h* ($GF14h^{Arroz}$) allele during seed
182 germination at low temperature (15°C) using *qLTG11*-NIL. RT-qPCR analysis of *GF14h*
183 expression levels showed that they were comparable in the embryo and endosperm at 1
184 and 3 days after the onset of seed imbibition (Fig 2D). At the beginning of germination,
185 when a white coleoptile was visible (5 and 7 days after seed imbibition), *GF14h*
186 expression levels rose in the endosperm, but not in the embryo (Fig 2D). By nine days of
187 imbibition, when most seeds had germinated, *GF14h* expression in the endosperm
188 returned to basal levels (Fig 2D). These results support the notion that *GF14h* plays a role

189 in seed germination at low temperature.

190

191 ## *GF14h* plays a vital role in LTG

192 To investigate the contribution of GF14h to LTG, we knocked out the functional *GF14h*
193 copy present in *qLTG11*-NIL by clustered regularly interspersed short palindromic repeat
194 (CRISPR)/CRISPR-associated nuclease 9 (Cas9)-mediated gene editing and evaluated
195 LTG. Specifically, we introduced two single guide RNA (sgRNA) constructs targeting the
196 exons of *GF14h* individually into *qLTG11*-NIL by Agrobacterium-mediated
197 transformation. We chose to knock out *GF14h* in the *qLTG11*-NIL background rather than
198 Arroz da Terra to evaluate the specific contribution of *GF14h* to LTG without the
199 influence of *qLTG3-1*, which would be present in the Arroz da Terra background. To
200 accurately evaluate the phenotypes of the edited plants, we selected heterozygous plants
201 in the T_0 generation and isolated homozygous mutant lines and their unedited
202 homozygous siblings in the T_1 generation. We obtained four knockout lines (*gf14h-1*,
203 *gf14h-2*, *gf14h-3*, and *gf14h-4*) and their wild-type sibling (WT^{Arroz}) (S9 Fig). We detected
204 significant drops in the germination percentage in all four knockout lines compared to
205 WT^{Arroz} (Fig 3A and 3B). We also found that the knockout lines tended to have lower
206 germination rates than WT^{Arroz} under normal temperature conditions (25°C) (S10 Fig),
207 which is consistent with the previous report [27]. Furthermore, we generated transgenic
208 lines in the Hitomebore background overexpressing the functional *GF14h* allele from
209 Arroz da Terra under the control of the CaMV 35S promoter. In these overexpression
210 lines, *GF14h* expression increased approximately 1,000-fold compared to the wild-type
211 sibling ($WT^{Hitomebore}$) (S11 Fig). Importantly, the overexpression lines showed higher LTG
212 than $WT^{Hitomebore}$ when tested at 15ºC (Fig 3C and 3D). Taken together, these data indicate

that *GF14h* is a key gene involved in LTG.

Loss-of-function alleles *GF14h* and *qLTG3-1* increased in frequency during rice breeding in Japan

We reconstructed the *GF14h* haplotype network using genotype data obtained from whole-genome resequencing of 492 *O. sativa* accessions from various collections, including the World Rice Core Collection [33], the Rice Core Collection of Japanese Landraces [34], and a set of Japanese landraces and modern varieties [35], in addition to 11 wild rice (*O. rufipogon*) accessions [36] (S2 Table). We distinguished 10 haplotypes for the *GF14h* coding region based on 11 polymorphic sites comprising one frameshift mutation caused by a 4-bp deletion, four nonsynonymous single nucleotide polymorphisms (SNPs), and six synonymous SNPs (S3 Table). The conversion of the functional allele Hap2 to its nonfunctional allele Hap1 required only a single step: a 4-bp deletion (S12 Fig).

We analyzed the haplotype frequencies of *GF14h* and *qLTG3-1* in Japanese landraces and cultivars, which we grouped according to their time of release. More than half of all Japanese landraces carried functional alleles of both *GF14h* and *LTG3-1* (Fig 4A). The next most common allele combination among the Japanese landraces was a nonfunctional *GF14h* allele with a functional *LTG3-1* allele (Fig 4A). The percentage of lines with loss-of-function alleles at both *GF14h* and *LTG3-1* has increased since the beginning of crossbreeding in Japan in the early 20th century, with more than 80% of varieties released after 2001 carrying loss-of-function alleles for both genes (Fig 4A and 4B). Looking at each gene separately in landraces, only a few lines carried a loss-of-

236 function allele for *LTG3-1*, whereas roughly half of all lines already harbored a loss-of-
237 function allele for *GF14h* (Fig 4B). Modern breeding thus appears to have increased the
238 proportion of loss-of-function alleles for these two genes, with a substantial increase in
239 *LTG3-1*, reaching almost 90% among lines bred after 2001 (Fig 4B).
240

241 ## The Arroz da Terra *GF14h* allele could be valuable for rice breeding

242 To assess how useful the above findings might be to practical breeding programs, we
243 developed new breeding materials. QTL pyramiding, a strategy for introducing multiple
244 QTLs for desired traits into a single genetic background, is a key strategy employed in
245 current breeding. An essential step in QTL pyramiding is the generation of NILs
246 containing the desired QTLs. Therefore, we developed a NIL, termed NIL-$GF14h^{Arroz}$,
247 using the elite cultivar Hitomebore as the genetic background into which we introgressed
248 a 172-kb region from the Arroz da Terra genome containing *GF14h* (S3 Fig). This NIL
249 showed a higher seed germination rate under low-temperature conditions compared to
250 Hitomebore (Fig 5A and 5B). In addition, although no significant difference was observed,
251 it is likely that NIL-$GF14h^{Arroz}$ tends to be more susceptible to pre-harvest sprouting than
252 Hitomebore (S13 Fig). Importantly, we observed no substantial differences in five
253 agronomic traits (culm length, panicle length, panicle number, grain number, and grain
254 weight) between NIL-$GF14h^{Arroz}$ and Hitomebore (Fig 5C–5G). Brown rice yield was
255 slightly lower in NIL-$GF14h^{Arroz}$ compared to Hitomebore, but a sufficient yield was
256 guaranteed (Fig 5H and 5I). These results suggest that NIL-$GF14h^{Arroz}$ could be a valuable
257 parental line for breeding via QTL pyramiding.
258

Discussion

Here, we demonstrated that the functional *GF14h* allele present in Portuguese rice variety Arroz da Terra plays a pivotal role in supporting seed germinability under low-temperature conditions. Although the regulation of seed germination by *GF14h* was recently documented, its activity under low-temperature conditions remained unclear [27, 28]. While many genomic regions associated with LTG have been detected through QTL mapping and GWAS, only a few studies have identified the causal genes [3-20]. Indeed, LTG is a quantitative trait involving the cumulative effects of multiple genes and their epistatic relationships, making it difficult to assess the specific effect of a single genomic region on LTG. To eliminate the influence of other chromosomal regions on LTG, we first generated *qLTG11*-NIL containing only one of three QTLs detected in the Arroz da Terra background for genetic analysis. The analysis of *qLTG11*-NIL revealed that *GF14h* participates in LTG. Significantly, the NIL harboring the functional *GF14h* allele from Arroz da Terra in the Hitomebore background provides valuable pre-breeding materials for QTL pyramiding. These findings provide a genetic understanding of low-temperature germinability as well as new resources for rice breeding.

Influence of *GF14h* on low-temperature germination

In this study, we identified *GF14h* as being implicated in LTG. In a previous study, a genetic complementation assay with a functional *GF14h* allele introduced into the rice cultivar Nipponbare background increased the germination rate at 30°C, but only to a limited extent at 15°C [28]. This result is not consistent with our finding that introducing functional *GF14h* into Hitomebore resulted in a significant improvement in germination

282 at low temperature. Perhaps this discrepancy is due to differences in the rice varieties
283 used in the germination assays. Notably, the haplotypes of *qLTG3-1*, a major QTL behind
284 LTG [3], are different between Nipponbare and Hitomebore: whereas Nipponbare, which
285 was released in 1961, harbors the functional allele of *qLTG3-1*, Hitomebore carries a loss-
286 of-function allele with a deletion of 71 bp (S2 Fig) [37]. Moreover, the cultivars
287 Koshihikari and Hayamasari, which carry the same loss-of-function *qLTG3-1* allele as
288 the Hitomebore variety, were reported to exhibit lower germination rates at low
289 temperatures than Nipponbare [37]. LTG tests using chromosome segment substitution
290 lines derived from a cross between Koshihikari and Nipponbare indicated that *qLTG3-1*
291 contributes to the difference in LTG between the two varieties [37]. Based on these
292 observations, it is likely that Nipponbare has a better LTG ability than Hitomebore, which
293 may have masked the effect of functional *GF14h* on LTG in the previous study [28]. Our
294 study confirmed the involvement of *GF14h* in LTG through map-based cloning and
295 analysis of knockout and overexpression lines. It is also worth mentioning that our
296 experiments were performed in the *qLTG11*-NIL background, which allowed us to isolate
297 the contribution of GF14h to LTG without any influence from *qLTG3-1* or other genes in
298 the Arroz da Terra background. In summary, we provided multiple lines of evidence that
299 *GF14h* contributes to LTG.

300 The expression pattern of functional *GF14h* during seed germination was
301 previously unclear. While *GF14h* has been shown to be expressed in the aleurone layer
302 surrounding the embryo [28], it is also highly expressed in the endosperm [27]. In the
303 current study, we showed that *GF14h* was expressed throughout the seeds, but with a
304 transient induction in expression in the endosperm at roughly the time of initiation of seed
305 germination. GF14h was reported to regulate seed germination by interacting with the

306 abscisic acid and gibberellin signaling pathways at optimal temperatures [27, 28]. We
307 therefore suggest that GF14h controls LTG by interacting with various phytohormone
308 signaling pathways.
309

310 Low-temperature germinability in rice was lost due to selection in
311 modern Japanese breeding

312 In this study, we performed haplotype network analysis of *GF14h* using many Japanese
313 rice varieties. We identified ten distinct haplotypes based on 11 polymorphic sites in the
314 *GF14h* coding region. Of these, Hap4, encompassing the aus, indica, tropical japonica,
315 temperate japonica, and *O. rufipogon* accessions, was defined at the center of the
316 haplotype network. Furthermore, we determined that a 4-bp deletion converted the
317 functional haplotype Hap2, which was derived from Hap4, into the nonfunctional
318 haplotype Hap1. This finding is consistent with the relationship between Hap6 and Hap1
319 (which we defined as Hap2 and Hap1, respectively) observed by [27]. These results
320 suggest that the nonfunctional allele represented by Hap1 was introduced into temperate
321 *japonica* varieties from tropical *japonica* varieties carrying Hap2 and then spread to
322 Japanese cultivars.

323 We studied the haplotype frequencies of *GF14h* and *qLTG3-1* in various Japanese
324 landraces and cultivars, considering their time of release from breeding programs into the
325 field. More than half of the Japanese landraces analyzed carried both functional *GF14h*
326 and *qLTG3-1* alleles. However, the frequency of varieties carrying loss-of-function alleles
327 for both *GF14h* and *qLTG3-1* has increased since crossbreeding began in the early 20th
328 century. This trend has continued to the present, perhaps as a result of artificial selection

329 to improve resistance to pre-harvest sprouting, with more than 80% of all varieties bred
330 since 2001 carrying these loss-of-function alleles.

331 Our study provides a historical perspective on allelic shifts in Japanese rice breeding
332 while highlighting the influence of modern breeding on genetic diversity. Further research
333 is needed to elucidate the potential effects of higher frequencies of loss-of-function alleles
334 on the overall phenotypic characteristics and ecological adaptability of Japanese rice
335 varieties. In addition, as mentioned in previous reports [27, 28], we believe that the
336 reintroduction of functional alleles should be considered in order to develop cultivars
337 suitable for labor-saving cultivation techniques such as direct seeding.

338

339 **Application to direct seeding for rice cultivation**

340 Cultivation stability under direct seeding conditions is important for managing rice
341 production costs and reducing labor. However, since rice is sensitive to low temperatures,
342 improving seed germination and seedling establishment at low temperatures is a desirable
343 breeding trait in high-latitude rice production areas such as Japan. In the current study,
344 we developed a potentially useful NIL (NIL-*GF14h*^{Arroz}) by introducing the functional
345 *GF14h* allele into the Hitomebore background. Overexpressing this functional *GF14h*
346 allele was previously shown to improve anaerobic germination and tolerance to seedling
347 establishment under anaerobic conditions in laboratory experiments [27]. However,
348 whether NIL-*GF14h*^{Arroz} exhibits strong seedling vigor at low temperatures in rice fields
349 remains to be determined. We previously identified a QTL associated with seedling vigor,
350 *qPHS3-2* (QTL for plant height of seedling 3-2) [38]. *qPHS3-2* most likely corresponds
351 to the gibberellin biosynthesis gene *GA20 oxidase1* (*OsGA20ox1*), a paralog of *Semi*
352 *Dwarf1* (*sd-1*, corresponding to *OsGA20ox2*) [38]. Therefore, the pyramiding of *qPHS3-*

2 in NIL-*GF14h*^{Arroz} by marker-assisted selection represents a promising approach for further improving seedling vigor in NIL-*GF14h*^{Arroz}. On the other hand, enhancing LTG may conversely increase the risk of pre-harvest sprouting. Should the level of pre-harvest sprouting in NIL-*GF14h*^{Arroz} pose practical issues, the pyramiding of QTLs for pre-harvest sprouting resistance, such as *Seed Dormancy 4* [39], may offer a solution.

In recent years, "early-winter direct seeding" has been experimentally tested as a new system of direct seeding for rice production in Japan [40]. In this system, seeds are directly sown in the early winter of the previous year instead of the spring. The sown seeds thus overwinter in snow-covered soil and germinate the following spring. The major advantage of this approach is that it can significantly decrease the amount of labor required by farmers during the busy spring season. However, it is challenging to overwinter the seeds of modern rice varieties in the soil and achieve good seedling establishment [40-42]. We expect that reintroducing beneficial alleles like *GF14h*^{Arroz} that were lost during modern breeding into future rice varieties will enable the implementation of new cultivation practices and increase productivity.

Materials and Methods

Plant materials

Rice was cultivated in a paddy field at Iwate Agricultural Research Center (39°35'N, 141°11'E). A recombinant inbred line (RIL) population of 200 F_7 lines was generated from a cross between Japanese variety Iwatekko and the high-LTG variety Arroz da Terra (S1 Fig) [31]. To develop NILs, rice cultivar Hitomebore was used as the recipient parent to generate NILs harboring the target genomic region from Arroz da Terra (S3A Fig),

thereby establishing *qLTG3-2*-NIL, *qLTG11*-NIL, and NIL-*GF14h*^{Arroz} (Fig 1E ; S3B and S4A Figs).

Evaluation of germination rate

Seeds for each line were harvested 45 days after heading, air-dried at 30°C for two days, and stored at 4°C until use. The seeds were air-dried at 50°C for seven days in the dark to break dormancy. For germination tests, 50 seeds per replicate were incubated in a Petri dish filled with distilled water in the dark at 15°C (low-temperature conditions) or 25°C (optimal temperature conditions). For QTL-seq analysis, germination tests were conducted at 13°C [31]. The germination rate was calculated as the total number of germinated seeds at each time point divided by the number of seeds tested. Seeds were considered to have germinated when the white coleoptile was visible.

To evaluate resistance to pre-harvest sprouting, panicles were harvested from NIL-*GF14h*^{Arroz} and Hitomebore 30 days after heading. The panicles were incubated in dark, wet conditions (by covering them with filter paper moistened with water) at 28°C for 10 days, and seed germination was scored.

QTL-seq analysis

LTG data for the 200 RILs derived from a cross between Iwatekko and Arroz da Terra (S1 Fig) were analyzed [31]. The top 20 RILs showing high-LTG and the bottom 20 RILs showing low-LTG phenotypes were selected to assemble the two bulk samples with contrasting LTG phenotypes. All seedlings with high or low LTG were pooled, and DNA was extracted from each bulk as previously described [31]. The genomic DNA of the two

399 bulks was used to generate DNA-seq libraries and sequenced on a GAIIx sequencer
400 (Illumina, CA, USA). QTL-seq was performed to identify QTLs related to LTG [31, 32].
401

402 ## Map-based cloning of *qLTG11*

403 To narrow down the *qLTG11* region, genotyping was performed using a cross population
404 of *qLTG11*-NIL (BC_2F_3) backcrossed to Hitomebore. The germination rate under low-
405 temperature conditions (15°C) was measured to characterize LTG activity. High-
406 resolution fine mapping with ten markers (markers B−K) between 23.466 Mb and 23.609
407 Mb on chromosome 11 identified six informative recombinants in the target region.
408 Primers used for mapping are listed in S4 Table.
409

410 ## *De novo* assembly of the Hitomebore and Arroz da Terra genomes

411 To reconstruct the *qLTG11* regions in Hitomebore and Arroz da Terra, *de novo* assembly
412 was performed for each genome using Nanopore long reads and Illumina short reads
413 according to a published method [43]. To extract high-molecular-weight genomic DNA
414 from leaf tissue for Nanopore sequencing, a NucleoBond high-molecular-weight DNA
415 kit (MACHEREY-NAGEL, Germany) was used. Following DNA extraction, low-
416 molecular-weight DNA was eliminated using a Short Read Eliminator Kit XL
417 (Circulomics, MD, USA). Library preparation was then performed using a Ligation
418 Sequencing Kit (SQK-LSK-109; Oxford Nanopore Technologies [ONT], United
419 Kingdom) according to the manufacturer's instructions, and sequencing was performed
420 using MinION (ONT, UK) for Arroz da Terra. For Hitomebore, Nanopore long reads
421 sequenced by [43] were used. Base-calling of the Nanopore long reads was performed

422 using Guppy 4.4.2 (ONT, UK). Sequences derived from the lambda phage genome were
423 removed from the raw reads with NanoLyse v1.1.0 [44]. The first 50 bp of each read were
424 then removed, as were reads with an average read quality score below 7 and reads shorter
425 than 3,000 bases, using NanoFilt v2.7.1 [44]. The clean Nanopore long reads were
426 assembled using NECAT v0.0.1 [45], setting the genome size to 380 Mb. To improve the
427 accuracy of assembly, Racon v1.4.20 [46] was used twice for error correction using
428 Nanopore reads, and Medaka v1.4.1 (https://github.com/nanoporetech/medaka) was
429 subsequently used to correct mis-assembly. Two rounds of consensus correction were
430 then performed using bwa-mem v0.7.17 [47] and HyPo v1.0.3 [48] with the Illumina
431 short reads. Redundant contigs were removed using purge-haplotigs v1.1.1 [49], resulting
432 in a *de novo* assembly of 374.8 Mb comprising 82 contigs for Hitomebore and 376.3 Mb
433 consisting of 82 contigs for Arroz da Terra. The resulting genome sequences have been
434 deposited in Zenodo (https://doi.org/10.5281/zenodo.10460309).
435

436 ## Plant transformation

437 To generate *GF14h* knockout mutants, two single guide RNAs (sgRNAs) targeting exon
438 4 or exon 5 of *GF14h* were designed using the web-based service CRISPRdirect
439 (crispr.dbcls.jp) [50] and cloned individually into the pZH::OsU6gRNA::MMCas9 vector
440 [51]. The resulting vectors were introduced into Agrobacterium (*Agrobacterium*
441 *tumefaciens*) strain EHA105 for transformation into *qLTG11*-NIL plants [52]. The target
442 sites in the positive transformants were sequenced by Sanger sequencing to detect
443 mutations. To obtain overexpression constructs, the full-length coding sequence of
444 functional *GF14h* was amplified from total RNA extracted from *qLTG11*-NIL and cloned
445 into the plant binary vector pCAMBIA1300 under the control of the cauliflower mosaic

446 virus (CaMV) 35S promoter. The overexpression plasmid was introduced into
447 Agrobacterium strain EHA105 for transformation of rice variety Hitomebore [52]. All
448 primers used are listed in S4 Table.
449

450 ## Expression analysis

451 Total RNA was extracted from germinating seeds using an RNA-suisui S kit (Rizo). Total
452 RNA was treated with RNase-free DNase I (Nippon Gene). The resulting samples were
453 reverse transcribed into first-strand cDNA using a PrimeScript RT Reagent Kit (Takara
454 Bio). Quantitative PCR (qPCR) was conducted using a QuantStudio 3 system (Thermo
455 Fisher Scientific) with Luna Universal qPCR Master Mix (New England Biolabs). The
456 cycling parameters were 1 min at 95°C, followed by 40 cycles of amplification (95°C for
457 15 sec and 60°C for 30 sec). The *Actin* gene (Os03g0718100) served as an internal control,
458 and the Delta CT method was used to calculate the relative expression levels. The primer
459 sets are listed in S4 Table.
460

461 ## RNA-seq

462 Total RNA was extracted from Hitomebore and *qLTG11*-NIL seeds at 0, 1, 2, and 3 days
463 after the onset of seed hydration under low (15°C) or optimum (25°C) temperature
464 conditions using an RNA-suisui S kit (Rizo, Ibaraki, Japan). Sequencing libraries were
465 prepared using an NEBNext Ultra II Directional RNA Library Prep Kit for Illumina (New
466 England Biolabs Japan, Tokyo, Japan) following the manufacturer's protocol. The
467 libraries were sequenced in paired-end mode using an Illumina HiSeq X instrument
468 (Illumina, CA, USA). The raw reads have been deposited in the DNA Databank of Japan

(BioProject accession No. PRJDB17450; S5 Table). For quality control, reads shorter than 50 bases and those with an average read quality below 20 were discarded using Trimmomatic v0.36 [53], and poly(A) sequences were trimmed using PRINSEQ++ v1.2 [54]. The resulting clean reads were aligned to the *de novo* assembled Hitomebore and Arroz da Terra genomes with HISAT2 v2.1 [55]. BAM files were sorted and indexed with SAMtools v1.10 [56], and aligned reads were assembled into transcripts with StringTie [57] by combining bam files for each variety. In a similar manner, the expression data were generated using the Nipponbare reference genome downloaded from IRGSP-1.0 (https://rapdb.dna.affrc.go.jp/download/irgsp1.html).

Haplotype network analysis

Sequencing datasets were obtained for 503 rice accessions. Of these, 379 were FASTQ files downloaded from the DNA Data Bank of Japan Sequence Read Archive (DRA) [33-35, 58] and 124 were sequenced in this study (S2 Table). Details about DNA extraction, whole-genome sequencing techniques, and construction of the genotype datasets in VCF format are provided in a previous report [35]. This study specifically focused on the coding region of *GF14h*. Genotype information related to the coding region of *GF14h* was extracted from the VCF dataset. In addition, the *k*-mer analysis program (https://github.com/taitoh1970/kmer) [59] was used with Illumina short reads to detect the 4-bp deletion with high sensitivity. Genotype information for the presence of the 4-bp deletion was added to the VCF file, and 81 samples with heterozygous genotypes were discarded. A haplotype network was then constructed using the median-joining network algorithm [60] implemented in Popart v1.7 [61].

Evaluation of agronomic traits and yield performance of NIL-*GF14h*^{Arroz}

The grain yields of Hitomebore and NIL-*GF14h*^{Arroz} were investigated in experimental paddy fields in 2023. Field experiments were conducted at the Iwate Agricultural Research Center (39°35'N, 141°11'E) in Kitakami, Iwate, Japan. A fertilization regime of $N:P_2O_5:K_2O$ = 6:6:6 g m^{-2} was applied as a basal dressing, and $N:K_2O$ = 2:2 g m^{-2} was applied as a top dressing. Seeds were sown in a seedling nursery box on 21 April, and seedlings were transplanted to the paddy field on 18 May. To evaluate agronomic traits, the seedlings were transplanted at a rate of one plant per hill, with a planting density of 22.2 hills m^{-2}. Culm length, panicle length, panicle number, grain number per plant, and grain weight per plant were measured at maturity. To evaluate yield performance, seedlings were transplanted with three plants per hill at a planting density of 16.7 hills m^{-2}. The 0.9 × 5.0 m experimental plots in the paddy fields were arranged in a randomized complete block design with three replicates. At maturity, 50 hills were harvested from each plot to measure brown rice yield. The hulls were removed using a rice huller (Model 25MC, Ohya Tanzo Factory Co., Ltd., Japan), and the hulled grains were screened with a grain sorter (1.9-mm sieve size). Brown rice yields were adjusted to 15% moisture content and converted to weight per hectare.

Acknowledgments

We thank the National Agriculture and Food Research Organization (NARO) gene bank, Japan, for providing rice seeds. This work was performed using the National Institute of Genetics (NIG) supercomputer at the Research Organization of Information and Systems

(ROIS) National Institute of Genetics and the Academic Center for Computing and Media Studies (ACCMS) supercomputer at Kyoto University.

Competing interests

None declared.

Author contributions

Conceptualization: Akira Abe, Hiroki Takagi, Ryohei Terauchi

Data curation: Yusaku Sugimura, Akira Abe

Formal analysis: Yusaku Sugimura, Yu Sugihara, Akira Abe

Funding acquisition: Akira Abe, Hiroki Takagi, Ryohei Terauchi

Investigation: Yusaku Sugimura, Akira Abe, Kaori Oikawa, Yu Sugihara, Hiroe Utsushi, Eiko Kanzaki, Kazue Ito, Yumiko Ogasawara, Tomoaki Fujioka, Hiroki Takagi, Motoki Shimizu, Hiroyuki Shimono

Supervision: Akira Abe, Ryohei Terauchi

Validation: Yusaku Sugimura, Akira Abe

Visualization: Yusaku Sugimura, Yu Sugihara, Akira Abe

Writing – original draft: Yusaku Sugimura, Akira Abe

Writing – review & editing: Yusaku Sugimura, Akira Abe, Ryohei Terauchi

References

1. Okuno K. Molecular Mechanisms of Cold Tolerance in Rice and Wheat. Thermal

538 Medicine(Japanese Journal of Hyperthermic Oncology). 2004;20(2):51-60. doi:
539 10.3191/thermalmedicine.20.51.
540 2. Iwata N, Shinada H, Kiuchi H, Sato T, Fujino K. Mapping of QTLs controlling
541 seedling establishment using a direct seeding method in rice. Breeding Science.
542 2010;60(4):353-60. doi: 10.1270/jsbbs.60.353.
543 3. Fujino K, Sekiguchi H, Matsuda Y, Sugimoto K, Ono K, Yano M. Molecular
544 identification of a major quantitative trait locus, qLTG3-1, controlling low-temperature
545 germinability in rice. Proc Natl Acad Sci U S A. 2008;105(34):12623-8. Epub 20080821.
546 doi: 10.1073/pnas.0805303105. PubMed PMID: 18719107; PubMed Central PMCID:
547 PMCPMC2527961.
548 4. Miura K, Lin SY, Yano M, Nagamine T. Mapping Quantitative Trait Loci
549 Controlling Low Temperature Germinability in Rice (Oryza sativa L.). Breeding Science.
550 2001;51(4):293-9. doi: 10.1270/jsbbs.51.293.
551 5. Fujino K, Sekiguchi H, Sato T, Kiuchi H, Nonoue Y, Takeuchi Y, et al. Mapping
552 of quantitative trait loci controlling low-temperature germinability in rice (Oryza sativa
553 L.). Theor Appl Genet. 2004;108(5):794-9. Epub 20031118. doi: 10.1007/s00122-003-
554 1509-4. PubMed PMID: 14624339.
555 6. Han LZ, Zhang YY, Qiao YL, Cao GL, Zhang SY, Kim JH, et al. Genetic and
556 QTL analysis for low-temperature vigor of germination in rice. Yi Chuan Xue Bao.
557 2006;33(11):998-1006. Epub 2006/11/23. doi: 10.1016/S0379-4172(06)60135-2.
558 PubMed PMID: 17112971.
559 7. Jiang L, Liu S, Hou M, Tang J, Chen L, Zhai H, et al. Analysis of QTLs for seed
560 low temperature germinability and anoxia germinability in rice (Oryza sativa L.). Field
561 Crops Research. 2006;98(1):68-75. doi: 10.1016/j.fcr.2005.12.015.

562 8. Nguyen HN, Park I-K, Yeo S-M, Yun Y-T, Ahn S-N. Mapping quantitative trait
563 loci controlling low-temperature germinability in rice. Korean Journal of Agricultural
564 Science. 2012;39(4):477-82. doi: 10.7744/cnujas.2012.39.4.477.
565 9. Li L, Liu X, Xie K, Wang Y, Liu F, Lin Q, et al. qLTG-9, a stable quantitative
566 trait locus for low-temperature germination in rice (Oryza sativa L.). Theor Appl Genet.
567 2013;126(9):2313-22. Epub 20130608. doi: 10.1007/s00122-013-2137-2. PubMed
568 PMID: 23748708.
569 10. Fujino K, Obara M, Shimizu T, Koyanagi KO, Ikegaya T. Genome-wide
570 association mapping focusing on a rice population derived from rice breeding programs
571 in a region. Breed Sci. 2015;65(5):403-10. Epub 20151201. doi: 10.1270/jsbbs.65.403.
572 PubMed PMID: 26719743; PubMed Central PMCID: PMCPMC4671701.
573 11. Pan Y, Zhang H, Zhang D, Li J, Xiong H, Yu J, et al. Genetic analysis of cold
574 tolerance at the germination and booting stages in rice by association mapping. PLoS One.
575 2015;10(3):e0120590. Epub 20150319. doi: 10.1371/journal.pone.0120590. PubMed
576 PMID: 25790128; PubMed Central PMCID: PMCPMC4366098.
577 12. Satoh T, Tezuka K, Kawamoto T, Matsumoto S, Satoh-Nagasawa N, Ueda K, et
578 al. Identification of QTLs controlling low-temperature germination of the East European
579 rice (Oryza sativa L.) variety Maratteli. Euphytica. 2015;207(2):245-54. doi:
580 10.1007/s10681-015-1531-z.
581 13. Jiang N, Shi S, Shi H, Khanzada H, Wassan GM, Zhu C, et al. Mapping QTL for
582 Seed Germinability under Low Temperature Using a New High-Density Genetic Map of
583 Rice. Front Plant Sci. 2017;8:1223. Epub 20170712. doi: 10.3389/fpls.2017.01223.
584 PubMed PMID: 28747923; PubMed Central PMCID: PMCPMC5506081.
585 14. Shakiba E, Edwards JD, Jodari F, Duke SE, Baldo AM, Korniliev P, et al. Genetic

586 architecture of cold tolerance in rice (Oryza sativa) determined through high resolution
587 genome-wide analysis. PLoS One. 2017;12(3):e0172133. Epub 20170310. doi:
588 10.1371/journal.pone.0172133. PubMed PMID: 28282385; PubMed Central PMCID:
589 PMCPMC5345765.
590 15. Wang X, Zou B, Shao Q, Cui Y, Lu S, Zhang Y, et al. Natural variation reveals
591 that OsSAP16 controls low-temperature germination in rice. J Exp Bot. 2018;69(3):413-
592 21. Epub 2017/12/14. doi: 10.1093/jxb/erx413. PubMed PMID: 29237030; PubMed
593 Central PMCID: PMCPMC5853544.
594 16. Jiang S, Yang C, Xu Q, Wang L, Yang X, Song X, et al. Genetic Dissection of
595 Germinability under Low Temperature by Building a Resequencing Linkage Map in
596 japonica Rice. Int J Mol Sci. 2020;21(4). Epub 20200214. doi: 10.3390/ijms21041284.
597 PubMed PMID: 32074988; PubMed Central PMCID: PMCPMC7072905.
598 17. Shim KC, Kim SH, Lee HS, Adeva C, Jeon YA, Luong NH, et al.
599 Characterization of a New qLTG3-1 Allele for Low-temperature Germinability in Rice
600 from the Wild Species Oryza rufipogon. Rice (N Y). 2020;13(1):10. Epub 20200205. doi:
601 10.1186/s12284-020-0370-2. PubMed PMID: 32025935; PubMed Central PMCID:
602 PMCPMC7002630.
603 18. Yang T, Zhou L, Zhao J, Dong J, Liu Q, Fu H, et al. The Candidate Genes
604 Underlying a Stably Expressed QTL for Low Temperature Germinability in Rice (Oryza
605 sativa L.). Rice (N Y). 2020;13(1):74. Epub 20201019. doi: 10.1186/s12284-020-00434-
606 z. PubMed PMID: 33074410; PubMed Central PMCID: PMCPMC7573065.
607 19. Pan Z, Tan B, Cao G, Zheng R, Liu M, Zeng R, et al. Integrative QTL
608 Identification, Fine Mapping and Candidate Gene Analysis of a Major Locus qLTG3a for
609 Seed Low-Temperature Germinability in Rice. Rice (N Y). 2021;14(1):103. Epub

610 20211215. doi: 10.1186/s12284-021-00544-2. PubMed PMID: 34910270; PubMed
611 Central PMCID: PMCPMC8674402.
612 20. Mao F, Wu D, Lu F, Yi X, Gu Y, Liu B, et al. QTL mapping and candidate gene
613 analysis of low temperature germination in rice (Oryza sativa L.) using a genome wide
614 association study. PeerJ. 2022;10:e13407. Epub 20220511. doi: 10.7717/peerj.13407.
615 PubMed PMID: 35578671; PubMed Central PMCID: PMCPMC9107303.
616 21. Morrison DK. The 14-3-3 proteins: integrators of diverse signaling cues that
617 impact cell fate and cancer development. Trends Cell Biol. 2009;19(1):16-23. Epub
618 20081120. doi: 10.1016/j.tcb.2008.10.003. PubMed PMID: 19027299; PubMed Central
619 PMCID: PMCPMC3073487.
620 22. Madeira F, Tinti M, Murugesan G, Berrett E, Stafford M, Toth R, et al. 14-3-3-
621 Pred: improved methods to predict 14-3-3-binding phosphopeptides. Bioinformatics.
622 2015;31(14):2276-83. Epub 20150303. doi: 10.1093/bioinformatics/btv133. PubMed
623 PMID: 25735772; PubMed Central PMCID: PMCPMC4495292.
624 23. Hermeking H. The 14-3-3 cancer connection. Nat Rev Cancer. 2003;3(12):931-
625 43. doi: 10.1038/nrc1230. PubMed PMID: 14737123.
626 24. Wilson RS, Swatek KN, Thelen JJ. Regulation of the Regulators: Post-
627 Translational Modifications, Subcellular, and Spatiotemporal Distribution of Plant 14-3-
628 3 Proteins. Front Plant Sci. 2016;7:611. Epub 20160509. doi: 10.3389/fpls.2016.00611.
629 PubMed PMID: 27242818; PubMed Central PMCID: PMCPMC4860396.
630 25. Camoni L, Visconti S, Aducci P, Marra M. 14-3-3 Proteins in Plant Hormone
631 Signaling: Doing Several Things at Once. Front Plant Sci. 2018;9:297. Epub 20180313.
632 doi: 10.3389/fpls.2018.00297. PubMed PMID: 29593761; PubMed Central PMCID:
633 PMCPMC5859350.

634 26. Chen F, Li Q, Sun L, He Z. The rice 14-3-3 gene family and its involvement in
635 responses to biotic and abiotic stress. DNA Res. 2006;13(2):53-63. Epub 20060421. doi:
636 10.1093/dnares/dsl001. PubMed PMID: 16766513.
637 27. Sun J, Zhang G, Cui Z, Kong X, Yu X, Gui R, et al. Regain flood adaptation in
638 rice through a 14-3-3 protein OsGF14h. Nat Commun. 2022;13(1):5664. Epub 20220929.
639 doi: 10.1038/s41467-022-33320-x. PubMed PMID: 36175427; PubMed Central PMCID:
640 PMCPMC9522936.
641 28. Yoshida H, Hirano K, Yano K, Wang F, Mori M, Kawamura M, et al. Genome-
642 wide association study identifies a gene responsible for temperature-dependent rice
643 germination. Nat Commun. 2022;13(1):5665. Epub 20220929. doi: 10.1038/s41467-022-
644 33318-5. PubMed PMID: 36175401; PubMed Central PMCID: PMCPMC9523024.
645 29. Ashikari M, Matsuoka M. Identification, isolation and pyramiding of
646 quantitative trait loci for rice breeding. Trends Plant Sci. 2006;11(7):344-50. doi:
647 10.1016/j.tplants.2006.05.008. PubMed PMID: 16769240.
648 30. Zhang B, Ma L, Wu B, Xing Y, Qiu X. Introgression Lines: Valuable Resources
649 for Functional Genomics Research and Breeding in Rice (Oryza sativa L.). Front Plant
650 Sci. 2022;13:863789. Epub 20220426. doi: 10.3389/fpls.2022.863789. PubMed PMID:
651 35557720; PubMed Central PMCID: PMCPMC9087921.
652 31. Takagi H, Abe A, Yoshida K, Kosugi S, Natsume S, Mitsuoka C, et al. QTL-seq:
653 rapid mapping of quantitative trait loci in rice by whole genome resequencing of DNA
654 from two bulked populations. Plant J. 2013;74(1):174-83. Epub 20130218. doi:
655 10.1111/tpj.12105. PubMed PMID: 23289725.
656 32. Sugihara Y, Young L, Yaegashi H, Natsume S, Shea DJ, Takagi H, et al. High-
657 performance pipeline for MutMap and QTL-seq. PeerJ. 2022;10:e13170. Epub 20220318.

658 doi: 10.7717/peerj.13170. PubMed PMID: 35321412; PubMed Central PMCID:
659 PMCPMC8935991.
660 33. Tanaka N, Shenton M, Kawahara Y, Kumagai M, Sakai H, Kanamori H, et al.
661 Whole-Genome Sequencing of the NARO World Rice Core Collection (WRC) as the
662 Basis for Diversity and Association Studies. Plant Cell Physiol. 2020;61(5):922-32. Epub
663 2020/02/27. doi: 10.1093/pcp/pcaa019. PubMed PMID: 32101292; PubMed Central
664 PMCID: PMCPMC7426033.
665 34. Tanaka N, Shenton M, Kawahara Y, Kumagai M, Sakai H, Kanamori H, et al.
666 Investigation of the Genetic Diversity of a Rice Core Collection of Japanese Landraces
667 using Whole-Genome Sequencing. Plant Cell Physiol. 2021;61(12):2087-96. doi:
668 10.1093/pcp/pcaa125. PubMed PMID: 33539537; PubMed Central PMCID:
669 PMCPMC7861467.
670 35. Shimono H, Abe A, Kim CH, Sato C, Iwata H. Upcycling rice yield trial data
671 using a weather-driven crop growth model. Commun Biol. 2023;6(1):764. Epub
672 20230721. doi: 10.1038/s42003-023-05145-x. PubMed PMID: 37479731; PubMed
673 Central PMCID: PMCPMC10362053.
674 36. Zhao Q, Feng Q, Lu H, Li Y, Wang A, Tian Q, et al. Pan-genome analysis
675 highlights the extent of genomic variation in cultivated and wild rice. Nat Genet.
676 2018;50(2):278-84. Epub 20180115. doi: 10.1038/s41588-018-0041-z. PubMed PMID:
677 29335547.
678 37. Hori K, Sugimoto K, Nonoue Y, Ono N, Matsubara K, Yamanouchi U, et al.
679 Detection of quantitative trait loci controlling pre-harvest sprouting resistance by using
680 backcrossed populations of japonica rice cultivars. Theor Appl Genet. 2010;120(8):1547-
681 57. Epub 20100210. doi: 10.1007/s00122-010-1275-z. PubMed PMID: 20145904;

682 PubMed Central PMCID: PMCPMC2859223.

683 38. Abe A, Takagi H, Fujibe T, Aya K, Kojima M, Sakakibara H, et al. OsGA20ox1,
684 a candidate gene for a major QTL controlling seedling vigor in rice. Theor Appl Genet.
685 2012;125(4):647-57. Epub 20120406. doi: 10.1007/s00122-012-1857-z. PubMed PMID:
686 22481119.

687 39. Sugimoto K, Takeuchi Y, Ebana K, Miyao A, Hirochika H, Hara N, et al.
688 Molecular cloning of Sdr4, a regulator involved in seed dormancy and domestication of
689 rice. Proc Natl Acad Sci U S A. 2010;107(13):5792-7. Epub 20100310. doi:
690 10.1073/pnas.0911965107. PubMed PMID: 20220098; PubMed Central PMCID:
691 PMCPMC2851884.

692 40. Shimono H. New technique : Early- winter direct- sowing cultivation in rice
693 under cool climate. Regulation of Plant Growth & Development. 2020;55(1):63-6. doi:
694 10.18978/jscrp.55.1_63.

695 41. Shimono H, Tamai M, Hamasaki T, Sagawa R, Ohtani R. Effects of Autumn
696 Direct-seeding on Rice Growth and Yield under Cool Climates. Japanese journal of crop
697 science. 2012;81(1):93-8. doi: 10.1626/jcs.81.93.

698 42. Oikawa S, Nishi M, Yui S, Kashiwagi J, Nakashima T, Ichikawa S, et al.
699 Improvement of Seedling Establishment by Seed Coating with Iron in Early-winter
700 Direct-sowing Rice. Japanese Journal of Crop Science. 2019;88(4):259-67. doi:
701 10.1626/jcs.88.259.

702 43. Sugihara Y, Abe Y, Takagi H, Abe A, Shimizu M, Ito K, et al. Disentangling the
703 complex gene interaction networks between rice and the blast fungus identifies a new
704 pathogen effector. PLoS Biol. 2023;21(1):e3001945. Epub 20230119. doi:
705 10.1371/journal.pbio.3001945. PubMed PMID: 36656825; PubMed Central PMCID:

706 PMCPMC9851567.

707 44. De Coster W, D'Hert S, Schultz DT, Cruts M, Van Broeckhoven C. NanoPack:
708 visualizing and processing long-read sequencing data. Bioinformatics.
709 2018;34(15):2666-9. doi: 10.1093/bioinformatics/bty149. PubMed PMID: 29547981;
710 PubMed Central PMCID: PMCPMC6061794.

711 45. Chen Y, Nie F, Xie SQ, Zheng YF, Dai Q, Bray T, et al. Efficient assembly of
712 nanopore reads via highly accurate and intact error correction. Nat Commun.
713 2021;12(1):60. Epub 20210104. doi: 10.1038/s41467-020-20236-7. PubMed PMID:
714 33397900; PubMed Central PMCID: PMCPMC7782737.

715 46. Vaser R, Sovic I, Nagarajan N, Sikic M. Fast and accurate de novo genome
716 assembly from long uncorrected reads. Genome Res. 2017;27(5):737-46. Epub 20170118.
717 doi: 10.1101/gr.214270.116. PubMed PMID: 28100585; PubMed Central PMCID:
718 PMCPMC5411768.

719 47. Li H, Durbin R. Fast and accurate short read alignment with Burrows-Wheeler
720 transform. Bioinformatics. 2009;25(14):1754-60. Epub 20090518. doi:
721 10.1093/bioinformatics/btp324. PubMed PMID: 19451168; PubMed Central PMCID:
722 PMCPMC2705234.

723 48. Kundu R, Casey J, Sung W-K. HyPo: Super Fast & Accurate Polisher for Long
724 Read Genome Assemblies. bioRxiv. 2019:2019.12.19.882506. doi:
725 10.1101/2019.12.19.882506.

726 49. Roach MJ, Schmidt SA, Borneman AR. Purge Haplotigs: allelic contig
727 reassignment for third-gen diploid genome assemblies. BMC Bioinformatics.
728 2018;19(1):460. Epub 20181129. doi: 10.1186/s12859-018-2485-7. PubMed PMID:
729 30497373; PubMed Central PMCID: PMCPMC6267036.

730 50. Naito Y, Hino K, Bono H, Ui-Tei K. CRISPRdirect: software for designing
731 CRISPR/Cas guide RNA with reduced off-target sites. Bioinformatics. 2015;31(7):1120-
732 3. Epub 20141120. doi: 10.1093/bioinformatics/btu743. PubMed PMID: 25414360;
733 PubMed Central PMCID: PMCPMC4382898.
734 51. Mikami M, Toki S, Endo M. Comparison of CRISPR/Cas9 expression constructs
735 for efficient targeted mutagenesis in rice. Plant Mol Biol. 2015;88(6):561-72. Epub
736 20150719. doi: 10.1007/s11103-015-0342-x. PubMed PMID: 26188471; PubMed
737 Central PMCID: PMCPMC4523696.
738 52. Toki S, Hara N, Ono K, Onodera H, Tagiri A, Oka S, et al. Early infection of
739 scutellum tissue with Agrobacterium allows high-speed transformation of rice. Plant J.
740 2006;47(6):969-76. doi: 10.1111/j.1365-313X.2006.02836.x. PubMed PMID: 16961734.
741 53. Bolger AM, Lohse M, Usadel B. Trimmomatic: a flexible trimmer for Illumina
742 sequence data. Bioinformatics. 2014;30(15):2114-20. Epub 20140401. doi:
743 10.1093/bioinformatics/btu170. PubMed PMID: 24695404; PubMed Central PMCID:
744 PMCPMC4103590.
745 54. Cantu VA, Sadural J, Edwards R. PRINSEQ++, a multi-threaded tool for fast
746 and efficient quality control and preprocessing of sequencing datasets. PeerJ Preprints.
747 2019;7:e27553v1. doi: 10.7287/peerj.preprints.27553v1.
748 55. Kim D, Paggi JM, Park C, Bennett C, Salzberg SL. Graph-based genome
749 alignment and genotyping with HISAT2 and HISAT-genotype. Nat Biotechnol.
750 2019;37(8):907-15. Epub 20190802. doi: 10.1038/s41587-019-0201-4. PubMed PMID:
751 31375807; PubMed Central PMCID: PMCPMC7605509.
752 56. Li H, Handsaker B, Wysoker A, Fennell T, Ruan J, Homer N, et al. The Sequence
753 Alignment/Map format and SAMtools. Bioinformatics. 2009;25(16):2078-9. Epub

754 20090608. doi: 10.1093/bioinformatics/btp352. PubMed PMID: 19505943; PubMed
755 Central PMCID: PMCPMC2723002.
756 57. Pertea M, Pertea GM, Antonescu CM, Chang TC, Mendell JT, Salzberg SL.
757 StringTie enables improved reconstruction of a transcriptome from RNA-seq reads. Nat
758 Biotechnol. 2015;33(3):290-5. Epub 20150218. doi: 10.1038/nbt.3122. PubMed PMID:
759 25690850; PubMed Central PMCID: PMCPMC4643835.
760 58. Yabe S, Yoshida H, Kajiya-Kanegae H, Yamasaki M, Iwata H, Ebana K, et al.
761 Description of grain weight distribution leading to genomic selection for grain-filling
762 characteristics in rice. PLoS One. 2018;13(11):e0207627. Epub 20181120. doi:
763 10.1371/journal.pone.0207627. PubMed PMID: 30458025; PubMed Central PMCID:
764 PMCPMC6245794.
765 59. Itoh T, Onuki R, Tsuda M, Oshima M, Endo M, Sakai H, et al. Foreign DNA
766 detection by high-throughput sequencing to regulate genome-edited agricultural products.
767 Sci Rep. 2020;10(1):4914. Epub 20200318. doi: 10.1038/s41598-020-61949-5. PubMed
768 PMID: 32188926; PubMed Central PMCID: PMCPMC7080720.
769 60. Bandelt HJ, Forster P, Rohl A. Median-joining networks for inferring
770 intraspecific phylogenies. Mol Biol Evol. 1999;16(1):37-48. doi:
771 10.1093/oxfordjournals.molbev.a026036. PubMed PMID: 10331250.
772 61. Leigh JW, Bryant D, Nakagawa S. popart: full‐feature software for haplotype
773 network construction. Methods in Ecology and Evolution. 2015;6(9):1110-6. doi:
774 10.1111/2041-210x.12410.
775 62. Cabanettes F, Klopp C. D-GENIES: dot plot large genomes in an interactive,
776 efficient and simple way. PeerJ. 2018;6:e4958. Epub 20180604. doi: 10.7717/peerj.4958.
777 PubMed PMID: 29888139; PubMed Central PMCID: PMCPMC5991294.

Figure legends

Fig 1. Effects of quantitative trait loci (QTLs) on low-temperature seed germinability.

(A) Representative photographs showing the germination of seeds from the Iwatekko, Hitomebore, and Arroz da Terra varieties 11 days (15°C) or 3 days (25°C) after the onset of seed imbibition. Scale bar, 1 cm. **(B–C)** Germination time courses of Iwatekko, Hitomebore, and Arroz da Terra at 15°C (B) or 25 °C (C). Values are means ± standard deviation (SD) from biologically independent samples (n = 8). Dunnett's test shows significant differences in germination for Hitomebore (upper) and Iwatekko (lower) compared with Arroz da Terra at each time point ($^{*}P < 0.05$, $^{**}P < 0.01$ and $^{***}P < 0.001$). **(D)** Map positions of QTLs for low-temperature germination, as determined by QTL-seq. The Δ (SNP-index) values (red lines) were plotted for chromosomes 3 and 11, with statistical confidence intervals under the null hypothesis of no QTL (green, $P < 0.05$; orange, $P < 0.01$). **(E)** Diagram showing the genotype of *qLTG11*-NIL. *qLTG11*-NIL harbors the Arroz da Terra allele at *qLTG11* on chromosome 11. Light blue indicates genomic fragments from Hitomebore; red indicates genomic fragments from Arroz da Terra; dark blue indicates heterozygous regions. **(F)** Germination time courses of Hitomebore and *qLTG11*-NIL at 15°C. Values are means ± SD from biologically independent samples (n = 10). Two-tailed t-test was used between *qLTG11*-NIL and Hitomebore for each time point ($^{*}P < 0.05$ and $^{***}P < 0.001$).

Fig 2. Positional cloning of *qLTG11*.

(A) Fine mapping of *qLTG11* to a 52-kb region between markers E and J. The chromosomal positions are based on the Nipponbare reference genome (Os-Nipponbare-Reference-IRGSP-1.0). Germination percentage was determined at 9 days of incubation at 15°C. Red and blue rectangles indicate chromosomal segments homozygous for Arroz da Terra or Hitomebore, respectively. Different lowercase letters indicate significant differences (n = 3 biologically independent samples, $P < 0.001$, Tukey's HSD test). **(B)** Genomic structure of the candidate genomic region in Arroz da Terra and Hitomebore. Os11g0609600 (shown in red), encoding GF14h, is expressed in germinating seeds. **(C)** Diagram of the *GF14h* gene structure and sequence polymorphisms between Arroz da Terra and Hitomebore. The chromosomal positions are based on the Nipponbare reference genome. The coding region of *GF14h* in Hitomebore is identical to that in Nipponbare. The 4-bp deletion in Hitomebore causes a frameshift and the introduction of a premature stop codon. **(D)** Relative *GF14h* expression levels in germinating seeds of *qLTG11*-NIL. This expression analysis was conducted by RT-qPCR. In the boxplots, the box edges represent the upper and lower quantiles, the horizontal line in the middle of the box represents the median value, whiskers represent the lowest quantile to the top quantile, and the black squares show the mean. Five biological replicates were measured independently. Different lowercase letters indicate significant differences based on Tukey's HSD test ($P < 0.05$). *OsActin1* (Os03g0718100) was used for normalization.

Fig 3. Effect of *GF14h* mutation and overexpression on low-temperature germination.

(A) Representative photographs showing seed germination in wild-type harboring Arroz-

type *GF14h* (WT^{Arroz}) and CRISPR/Cas9 knockout lines (*gf14-1*) at 8 days after the onset of seed imbibition. Scale bar, 1 cm. **(B)** Seed germination rate of WT^{Arroz} and its CRISPR/Cas9 knockout lines at 7 days of seed imbibition at 15°C. The two target constructs (S9 Fig) were introduced into the *qLTG11*-NIL line. Data are means ± standard error (SE, $n = 3$). Different lowercase letters indicate significant differences based on Tukey's HSD test ($P < 0.01$). **(C)** Representative photographs showing seed germination of wild-type ($WT^{Hitomebore}$) and $OsGF14h^{Arroz}$ overexpression lines ($OsGF14h^{Arroz}$-Ox #2) at 7 days of seed imbibition at 15ºC. Scale bar, 1 cm. **(D)** Seed germination rate of $WT^{Hitomebore}$ and $GF14h^{Arroz}$ overexpression lines in the Hitomebore background at 7 days of seed imbibition at 15°C. Data are means ± SE ($n = 3$). Different lowercase letters indicate significant differences based on Tukey's HSD test ($P < 0.05$).

Fig 4. Gradual selection of loss-of-function alleles in *GF14h* and *qLTG3-1* during rice breeding in Japan.

A total of 350 Japanese varieties were examined, including the World Rice Core Collection [33], the Rice Core Collection of Japanese Landraces [34], and the collection of Japanese core cultivars [35]. The allele type at each gene was determined to be functional or nonfunctional by the k-mer method using Illumina short reads for each variety. **(A)** Proportion of allele type combinations at *GF14h* and *qLTG3-1* sorted by breeding year. **(B)** Proportion of nonfunctional allele types at *GF14h* and *qLTG3-1* sorted by breeding year.

Fig 5. Phenotypic analysis of a near-isogenic line homozygous for Arroz-type *GF14h* in the Hitomebore genetic background (NIL-$GF14h^{Arroz}$).

(A) Gross morphology of Hitomebore and NIL-*GF14h*^{Arroz} at 87 days after transplanting (top row), and seed germination at 9 days after the onset of seed imbibition at 15°C (bottom row). Scale bars, 20 cm (top), 1 cm (bottom). **(B)** Low-temperature germination ability of NIL-*GF14h*^{Arroz} at 8 days after the onset of seed imbibition at 15°C. Values are means ± SE of biologically independent samples (n = 3). Asterisks indicate significant differences, as determined by two-tailed t-test. **(C–G)** Agronomic traits in Hitomebore and NIL-*GF14h*^{Arroz}: culm length (**C**), panicle length (**D**), panicle number (**E**), grain number per plant (**F**), and grain weight per plant (**G**). Values are means ± SE of biologically independent plants (n = 40). **(H)** Side view of Hitomebore and NIL-*GF14h*^{Arroz} growing in the field under typical rice-growing conditions at the maturity stage. **(I)** Brown rice yield per unit area. Values are means ± SE of biologically independent plots (n = 3). P-values calculated by t-tests are listed throughout the figure.

Supporting information

S1 Fig. Frequency distribution of germination rates in the RIL population and germination rates of selected RILs for QTL-seq analysis.

(A) Frequency distribution of germination rates at 13°C after eight days from seed imbibition in 200 F7 RILs derived from a cross between Iwatekko and Arroz da Terra [31]. **(B)** Selection of RILs with low cold germination rates. The 62 RILs with the lower germination rates from the first test (A) were tested for the second, and then the 20 RILs with the lowest germination rates were selected as a bulk sample for QTL-seq analysis. The bar graph shows the mean values of the two tests. **(C)** Selection of RILs with high cold germination rates. The 37 RILs with the higher germination rates from the first test

(A) were tested for the second, and then the 20 RILs with the highest germination rates were selected for a bulk sample for QTL-seq analysis. The bar graph shows the average values of the two tests.

S2 Fig. Multiple DNA sequence alignment of *qLTG3-1* variants.

Arroz da Terra and Italica Livorno harbor a functional *qLTG3-1* variant. Nipponbare carries another functional *qLTG3-1* variant due to the nonsynonymous substitution (*). Iwatekko, Hitomebore, and Hayamasari contain a loss-of-function variant for *qLTG3-1* due to a 71-bp deletion.

S3 Fig. Generation of a near-isogenic line with high LTG in the Hitomebore background.

(A) Strategy for the development of *qLTG3-2*-NIL, *qLTG11*-NIL, and NIL-*GF14h*^{Arroz}. Molecular markers were used for foreground and background selection. **(B)** Diagram showing the genotype of NIL-*GF14h*^{Arroz}. NIL-*GF14h*^{Arroz} contains a 172-kb region on chromosome 11 harboring the Arroz da Terra allele of *GF14h*. Light blue bars indicate genomic fragments from Hitomebore; red bars indicate genomic fragments from Arroz da Terra.

S4 Fig. Summary of *qLTG3-2*.

(A) Diagram showing the genotype of *qLTG3-2*-NIL containing the Arroz da Terra allele at *qLTG3-2* on chromosome 3. Light blue bars indicate genomic fragments from Hitomebore; red bars indicate genomic fragments from Arroz da Terra; dark blue bars indicate heterozygous regions. **(B)** Germination time courses for seeds of Hitomebore,

the *qLTG3-2*-NIL, and Arroz da Terra at 15°C. Values are means ± SD of biologically independent samples (Hitomebore and NIL $n = 10$, Arroz da Terra $n = 5$).

S5 Fig. Seed germination of *qLTG11*-NIL under optimal temperature conditions. Germination time courses of seeds from Hitomebore and *qLTG11*-NIL at 25°C. Values are means ± SD of biologically independent samples ($n = 3$). Two-tailed t-test was used between *qLTG11*-NIL and Hitomebore for each time point (*$P < 0.05$ and **$P < 0.01$).

S6 Fig. Comparison of the *qLTG11* genomic region in Hitomebore, Arroz da Terra, and Nipponbare. Dot blot analyses of the genomic sequence in the *qLTG11* candidate region between **(A)** Hitomebore and Nipponbare and **(B)** Hitomebore and Arroz da Terra, using D-GENIES [62]. Based on the Nipponbare genome (IRGSP-1.0), the genomic region containing the causative gene is located at 23.512–23.564 Mb (approximately 52 kb) on chromosome 11. The genome sequence of Hitomebore is identical to that of Nipponbare. The candidate region corresponds to a fragment of approximately 94 kb in the Arroz da Terra genome.

S7 Fig. Expression levels of the two annotated genes in the candidate genomic region of *qLTG11* based on RNA-seq data. Total RNA was extracted from Hitomebore and *qLTG11*-NIL seeds at 0, 1, 2, and 3 days after the onset of seed imbibition under 15 or 25°C temperature conditions, followed by RNA-seq. The sequence reads were mapped to the Nipponbare genome (IRGSP-1.0), and expression data were obtained. **(A–B)** The expression levels of Os11g0609600 (*GF14h*) during seed germination under 15°C (A) and 25°C (B) are shown. Data are presented as

means ± SE. n = 3 biologically independent samples. **(C–D)** The expression levels of Os11g0609500 (*Jacalin-like lectin domain containing protein*) during seed germination under 15°C (C) and 25°C (D) are shown. Data are presented as means ± SE. n = 3 biologically independent samples.

S8 Fig. Multiple DNA sequence alignment of *GF14h* variants.

Arroz da Terra carries a functional *GF14h* variant. Hitomebore and Nipponbare harbors a loss-of-function variant of *GF14h* due to a 4-bp deletion (black line).

S9 Fig. CRISPR/Cas9-mediated genome editing of *GF14h*.

Top, diagram showing the *GF14h* locus, with the locations of the two sgRNA target sites marked by inverted red triangles. Bottom, sequencing results of putative *gf14h* mutants. The sgRNA target sites are underlined, and the PAMs are highlighted. The mutation sites in $GF14h^{Arroz}$ for the four mutants (*gf14h-1*, *gf14h-2*, *gf14h-3,* and *gf14h-4*) are indicated.

S10 Fig. Effect of *GF14h* mutation on optimal-temperature germination.

(A) Representative photographs showing seed germination in wild-type harboring Arroz-type *GF14h* (WT^{Arroz}) and CRISPR/Cas9 knockout lines (*gf14-1*) at 3 days after the onset of seed imbibition. Scale bar, 1 cm. **(B)** Seed germination rate of WT^{Arroz} and its CRISPR/Cas9 knockout lines at 2 days of seed imbibition at 25°C. The two target constructs (S9 Fig) were introduced into the *qLTG11*-NIL line. Data are means ± standard error (WT^{Arroz}, *gf14h-1*, *gf14h-2* and *gf14h-4*, n = 3; *gf14h-3*, n = 2). Different lowercase letters indicate significant differences based on Tukey's HSD test ($P < 0.05$).

S11 Fig. Relative *GF14h* expression levels in germinating seeds of *GF14h^{Arroz}* overexpression lines and the parental line.

The *GF14h^{Arroz}* overexpression construct was introduced into Hitomebore. *OsActin1* (Os03g0718100) was used for normalization. Values are means ± SE (n = 3 or 4). Different lowercase letters indicate significant differences based on Tukey's HSD test (P < 0.001).

S12 Fig. Haplotype network of *GF14h*.

The *GF14h* genomic sequences obtained from 411 *O. sativa* varieties and 11 *O. rufipogon* accessions were used for analysis (S1 Table). The haplotype network was reconstructed by the median joining network algorithm [60] implemented in Popart v1.7 [61]. The haplotype Hap1 evolved from Hap2 by acquiring the 4-bp sequence, resulting in a nonfunctional *GF14h* gene. The Hitomebore cultivar contains Hap1 (nonfunctional), and the Arroz da Terra cultivar contains Hap9 (functional).

S13 Fig. Pre-harvest sprouting of NIL-*GF14h^{Arroz}*.

Germination time courses of seeds from Hitomebore (blue circles) and the NIL-*GF14h^{Arroz}* (pink triangles) under wet conditions at 28°C. Seeds were harvested from tagged panicles 30 days after heading. Values are means ± SE of biologically independent samples (n = 3). The P-values calculated from t-tests at each time point are shown in the figure.

S14 Fig. Development of a functional marker based on the 4-bp deletion in *GF14h*.

(A) Diagram of the sequence around the 4-bp InDel of *GF14h*. In the Hitomebore (loss-

968 of-function) allele, the 4-bp deletion creates a SmlI restriction site. **(B)** Genotyping of the
969 4-bp deletion in *GF14h*. A genomic fragment containing the 4-bp InDel of *GF14h* was
970 amplified by PCR and digested with SmlI. The products were separated on a 3% (w/v)
971 agarose gel and stained with Midori Green. The PCR product from $GF14h^{Arroz}$
972 (approximately 500 bp) was not cleaved, whereas the PCR product from $GF14h^{Hitomebore}$
973 was cleaved, producing two fragments of approximately 250 bp each. Both bands were
974 detected in heterozygous plants.
975
976 **S1 Table. Expression profile (TPM) during seed germination by RNA-seq.**
977
978 **S2 Table. List of rice varieties used in this study and their sequence read archive**
979 **(SRA) IDs.**
980
981 **S3 Table. Haplotypes of the *GF14h* gene analyzed in S12 Fig.**
982
983 **S4 Table. Primers used in this study.**
984
985 **S5 Table. List of RNA-seq samples used in this study and their sequence read archive**
986 **(SRA) IDs.**
987

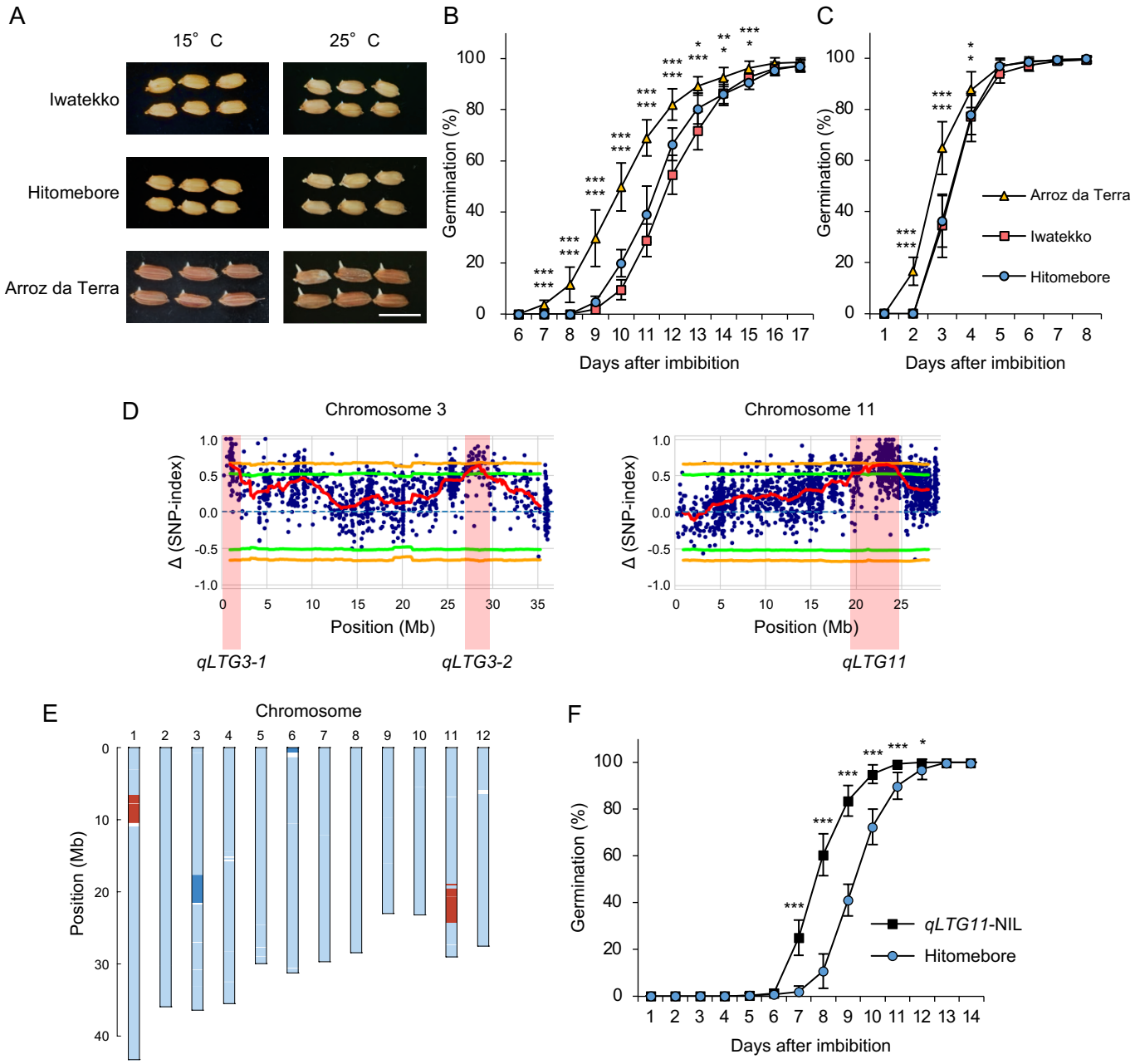

Fig 1. Effects of quantitative trait loci (QTLs) on low-temperature seed germinability.
(A) Representative photographs showing the germination of seeds from the Iwatekko, Hitomebore, and Arroz da Terra varieties 11 days (15° C) or 3 days (25° C) after the onset of seed imbibition. Scale bar, 1 cm. **(B–C)** Germination time courses of Iwatekko, Hitomebore, and Arroz da Terra at 15° C (B) or 25 ° C (C). Values are means ± standard deviation (SD) from biologically independent samples ($n = 8$). Dunnett's test shows significant differences in germination for Hitomebore (upper) and Iwatekko (lower) compared with Arroz da Terra at each time point ($^{*}P < 0.05$, $^{**}P < 0.01$ and $^{***}P < 0.001$). **(D)** Map positions of QTLs for low-temperature germination, as determined by QTL-seq. The Δ (SNP-index) values (red lines) were plotted for chromosomes 3 and 11, with statistical confidence intervals under the null hypothesis of no QTL (green, $P < 0.05$; orange, $P < 0.01$). **(E)** Diagram showing the genotype of *qLTG11*-NIL. *qLTG11*-NIL harbors the Arroz da Terra allele at *qLTG11* on chromosome 11. Light blue indicates genomic fragments from Hitomebore; red indicates genomic fragments from Arroz da Terra; dark blue indicates heterozygous regions. **(F)** Germination time courses of Hitomebore and *qLTG11*-NIL at 15° C. Values are means ± SD from biologically independent samples ($n = 10$). Two-tailed t-test was used between *qLTG11*-NIL and Hitomebore for each time point ($^{*}P < 0.05$ and $^{***}P < 0.001$).

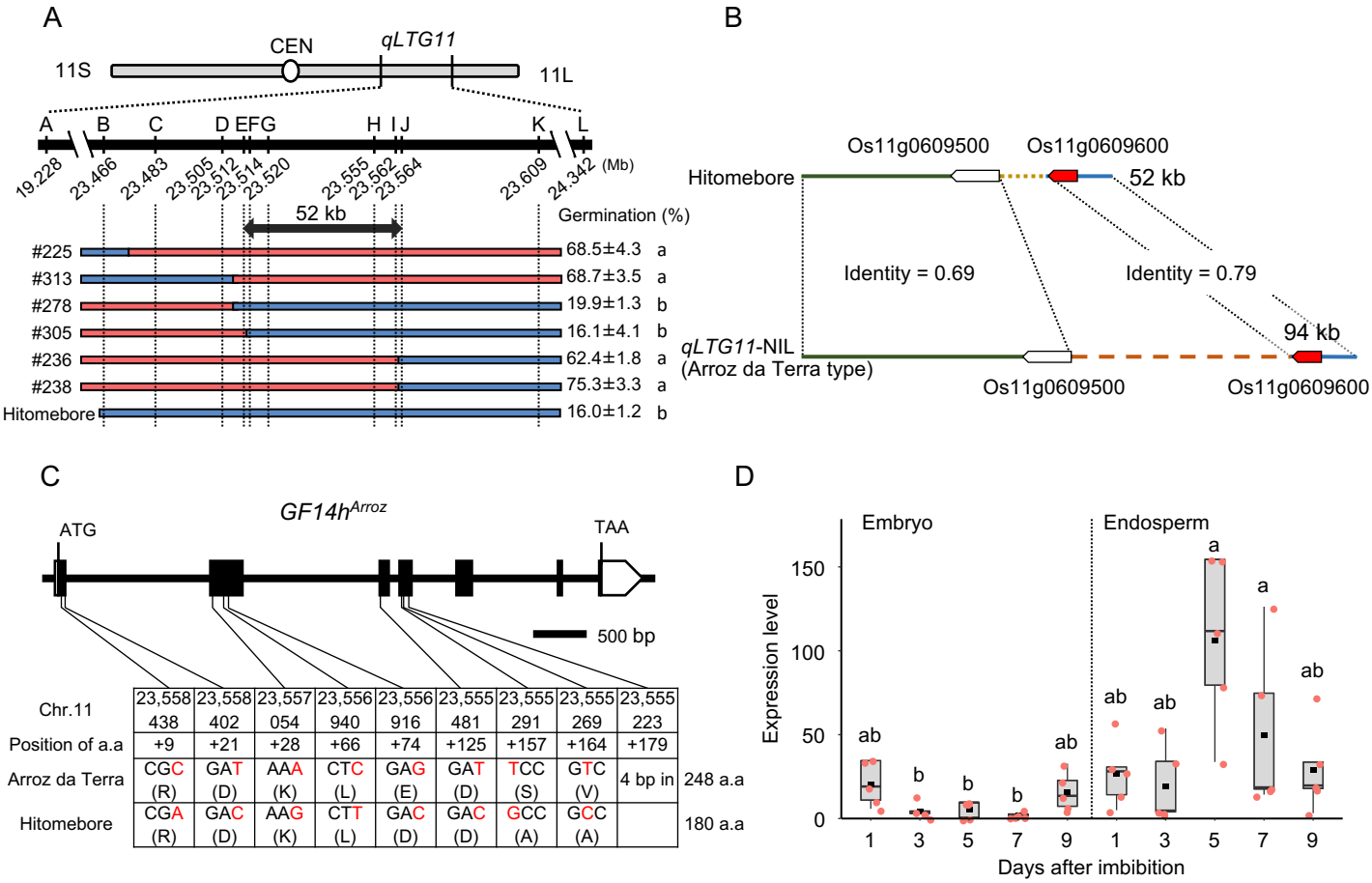

Fig 2. Positional cloning of *qLTG11*.

(A) Fine mapping of *qLTG11* to a 52-kb region between markers E and J. The chromosomal positions are based on the Nipponbare reference genome (Os-Nipponbare-Reference-IRGSP-1.0). Germination percentage was determined at 9 days of incubation at 15° C. Red and blue rectangles indicate chromosomal segments homozygous for Arroz da Terra or Hitomebore, respectively. Different lowercase letters indicate significant differences ($n = 3$ biologically independent samples, $P < 0.001$, Tukey's HSD test). **(B)** Genomic structure of the candidate genomic region in Arroz da Terra and Hitomebore. Os11g0609600 (shown in red), encoding GF14h, is expressed in germinating seeds. **(C)** Diagram of the *GF14h* gene structure and sequence polymorphisms between Arroz da Terra and Hitomebore. The chromosomal positions are based on the Nipponbare reference genome. The coding region of *GF14h* in Hitomebore is identical to that in Nipponbare. The 4-bp deletion in Hitomebore causes a frameshift and the introduction of a premature stop codon. **(D)** Relative *GF14h* expression levels in germinating seeds of *qLTG11*-NIL. This expression analysis was conducted by RT-qPCR. In the boxplots, the box edges represent the upper and lower quantiles, the horizontal line in the middle of the box represents the median value, whiskers represent the lowest quantile to the top quantile, and the black squares show the mean. Five biological replicates were measured independently. Different lowercase letters indicate significant differences based on Tukey's HSD test ($P < 0.05$). *OsActin1* (Os03g0718100) was used for normalization.

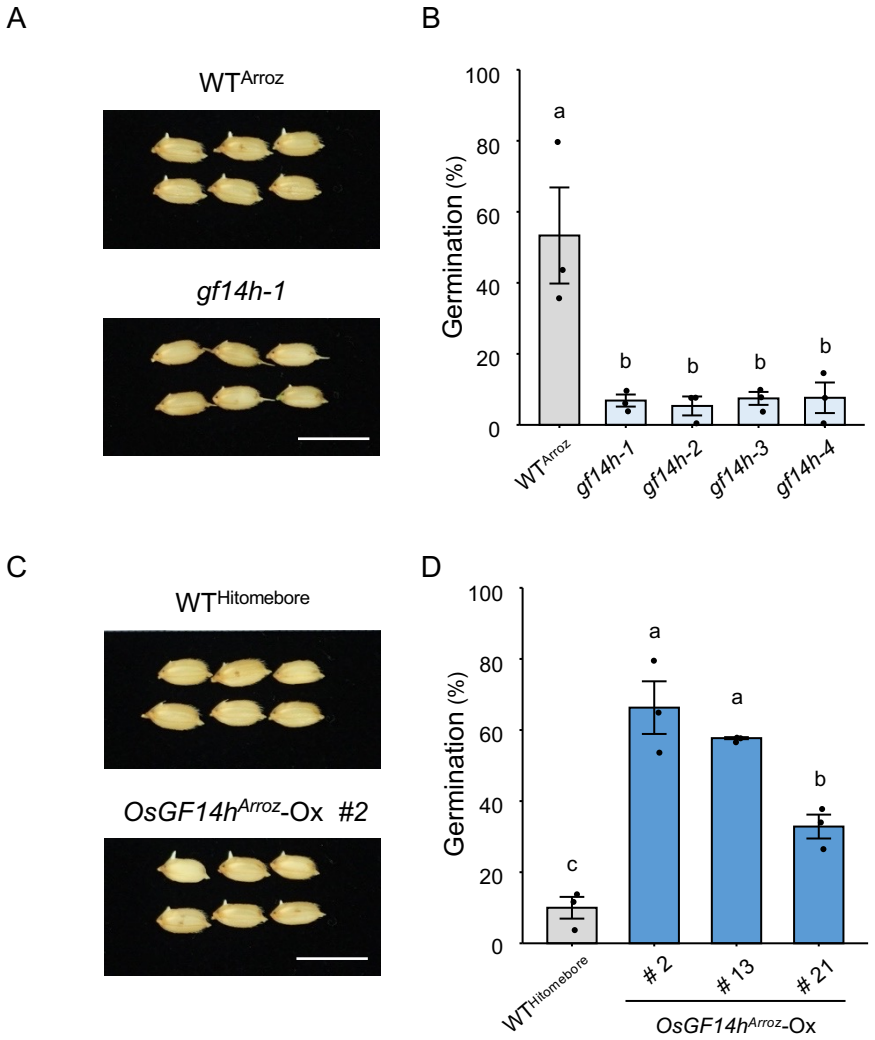

Fig 3. Effect of *GF14h* mutation and overexpression on low-temperature germination. **(A)** Representative photographs showing seed germination in wild-type harboring Arroz-type *GF14h* (WT^{Arroz}) and CRISPR/Cas9 knockout lines (*gf14-1*) at 8 days after the onset of seed imbibition. Scale bar, 1 cm. **(B)** Seed germination rate of WT^{Arroz} and its CRISPR/Cas9 knockout lines at 7 days of seed imbibition at 15° C. The two target constructs (S9 Fig) were introduced into the *qLTG11*-NIL line. Data are means ± standard error (SE, $n = 3$). Different lowercase letters indicate significant differences based on Tukey's HSD test ($P < 0.01$). **(C)** Representative photographs showing seed germination of wild-type ($WT^{Hitomebore}$) and $OsGF14h^{Arroz}$ overexpression lines ($OsGF14h^{Arroz}$-Ox #2) at 7 days of seed imbibition at 15ºC. Scale bar, 1 cm. **(D)** Seed germination rate of $WT^{Hitomebore}$ and $GF14h^{Arroz}$ overexpression lines in the Hitomebore background at 7 days of seed imbibition at 15° C. Data are means ± SE ($n = 3$). Different lowercase letters indicate significant differences based on Tukey's HSD test ($P < 0.05$).

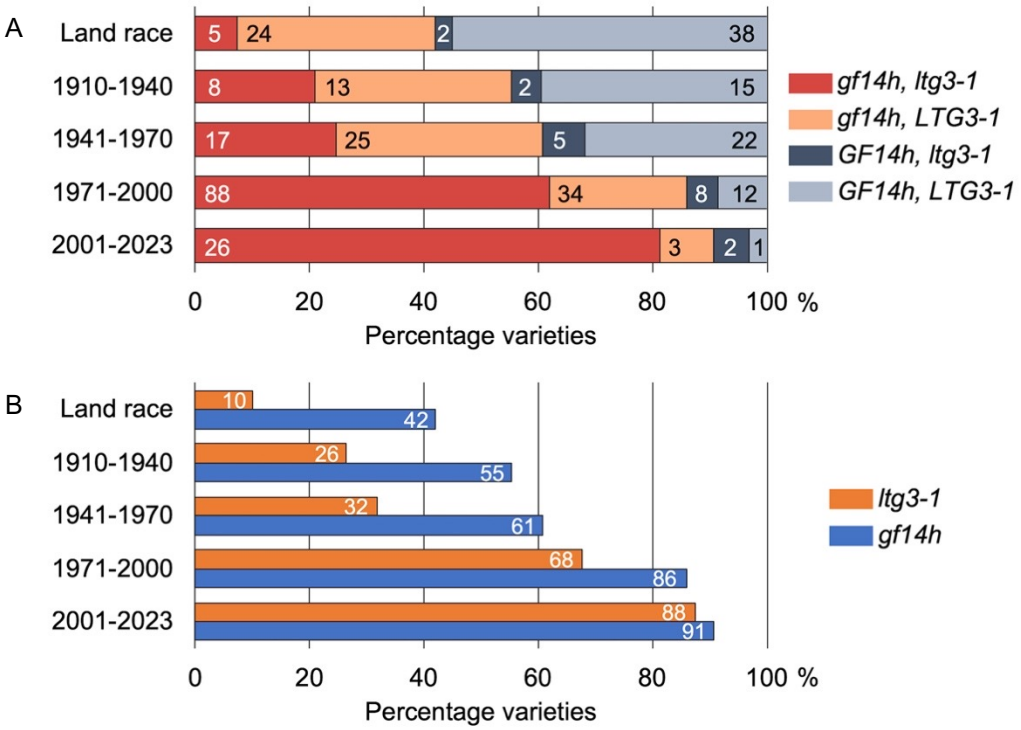

Fig 4. Gradual selection of loss-of-function alleles in *GF14h* and *qLTG3-1* during rice breeding in Japan.

A total of 350 Japanese varieties were examined, including the World Rice Core Collection [33], the Rice Core Collection of Japanese Landraces [34], and the collection of Japanese core cultivars [35]. The allele type at each gene was determined to be functional or nonfunctional by the k-mer method using Illumina short reads for each variety. **(A)** Proportion of allele type combinations at *GF14h* and *qLTG3-1* sorted by breeding year. **(B)** Proportion of nonfunctional allele types at *GF14h* and *qLTG3-1* sorted by breeding year.

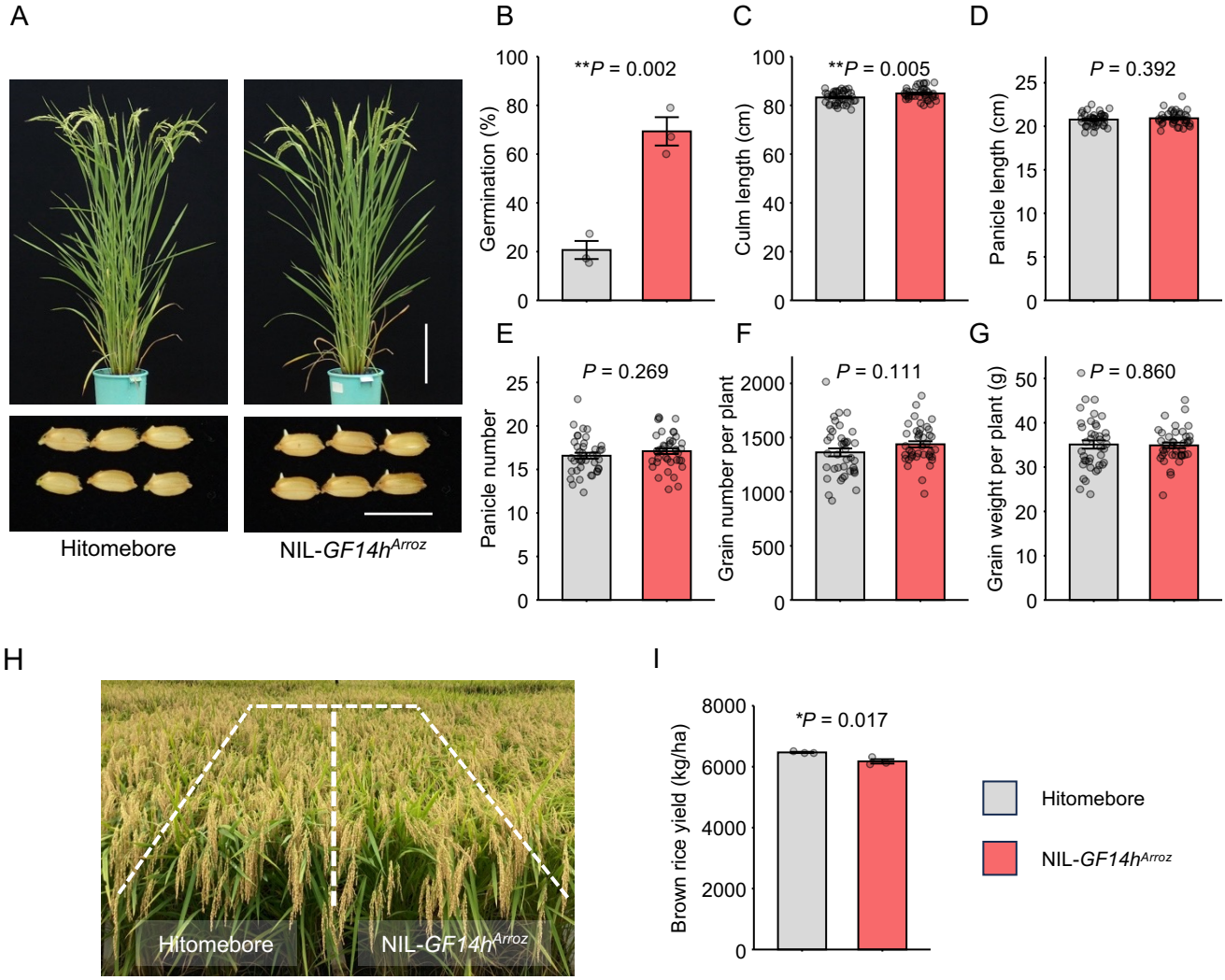

Fig 5. Phenotypic analysis of a near-isogenic line homozygous for Arroz-type *GF14h* in the Hitomebore genetic background (NIL-*GF14h*^{Arroz}).

(A) Gross morphology of Hitomebore and NIL-*GF14h*^{Arroz} at 87 days after transplanting (top row), and seed germination at 9 days after the onset of seed imbibition at 15° C (bottom row). Scale bars, 20 cm (top), 1 cm (bottom). **(B)** Low-temperature germination ability of NIL-*GF14h*^{Arroz} at 8 days after the onset of seed imbibition at 15° C. Values are means ± SE of biologically independent samples (n = 3). Asterisks indicate significant differences, as determined by two-tailed t-test. **(C–G)** Agronomic traits in Hitomebore and NIL-*GF14h*^{Arroz}: culm length (**C**), panicle length (**D**), panicle number (**E**), grain number per plant (**F**), and grain weight per plant (**G**). Values are means ± SE of biologically independent plants (n = 40). **(H)** Side view of Hitomebore and NIL-*GF14h*^{Arroz} growing in the field under typical rice-growing conditions at the maturity stage. **(I)** Brown rice yield per unit area. Values are means ± SE of biologically independent plots (n = 3). P-values calculated by t-tests are listed throughout the figure.